ACS Catalysis

Research Article

pubs.acs.org/acscatalysis

Mechanistic Exploration of the Pd-Catalyzed Copper-Free Sonogashira Reaction

Max García-Melchor,[†] María C. Pacheco,[‡] Carmen Nájera,*[,‡] Agustí Lledós,*[,†] and Gregori Ujaque*[,†]

[†]Departament de Química, Edifici Cn, Universitat Autònoma de Barcelona, E-08193 Cerdanyola del Vallès, Catalonia, Spain

[‡]Departamento de Química Orgánica, Universidad de Alicante, Apartado 99, E-03080 Alicante, Spain

Supporting Information

ABSTRACT: The reaction mechanism for the Pd-catalyzed Cu-free Sonogashira reaction is analyzed by means of density functional theory (DFT) calculations on a model system. The most common routes proposed in the literature for this reaction, namely, the carbopalladation and deprotonation, are considered. In agreement with experiment, calculations clearly demonstrate that the carbopalladation route can be discarded. For the case of the deprotonation route, however, the reaction pathway may take place via several alternatives; calculations suggest that all of them are feasible. Moreover, an additional pathway where the halide is initially replaced by the base in the coordination sphere of the catalyst is found to be also competitive. The effects of the alkyne's substituents on the reaction are also analyzed by a combined computational and experimental work. Theoretical results suggest that these effects are rather small, and they are confirmed by experiments.

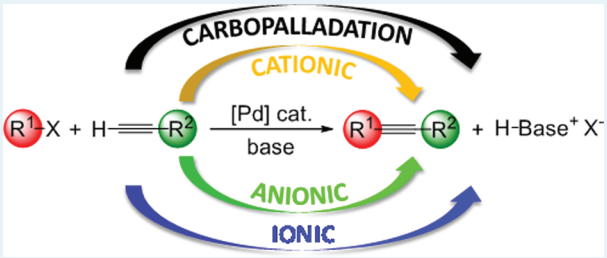

KEYWORDS: *cross-coupling reactions, Sonogashira reaction, DFT calculations, palladium, alkynes*

1. INTRODUCTION

The palladium-catalyzed Sonogashira reaction is one of the most important and widely used methods for preparing arylacetylenes and conjugated enynes,[1−6] which are precursors for natural products, pharmaceuticals, and materials with specialized optical and electronic properties.[6−12] The general Sonogashira protocol for the coupling of terminal alkynes with aryl or alkenyl halides (or triflates) usually involves an organic solvent, a Pd(0)/Cu(I) catalytic system, and at least a stoichiometric amount of a base (Scheme 1).[13] The presence

Scheme 1. General Pd-Catalyzed Sonogashira Reaction

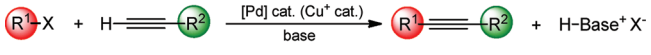

R^1= aryl, hetaryl, alkenyl, alkyl, SiR_3
R^2= aryl, hetaryl, vinyl
X= I, Br, Cl, OTf

of a copper(I) salt as cocatalyst in the typical Sonogashira reaction is generally believed to facilitate the reaction by the in situ generation of copper acetylide. However, the addition of this copper(I) salt under the reaction conditions entails some drawbacks,[14,15] mainly the induction of the so-called Glaser-type oxidative homocoupling of the terminal alkyne to yield the diyne.[16,17] Aiming at the suppression of the formation of this byproduct, many efforts have been devoted to develop reaction procedures working in the absence of copper salts.[18−26] All these copper-free strategies are commonly known as copper-free Sonogashira reaction. Unfortunately, this copper-free variant frequently requires the use of an excess of amine (often even acting as solvent), which proves detrimental to the environmental and economical advantages of this methodology. To avoid that, several modifications of the original Sonogashira reaction have been recently reported including amine-free, ligand-free, and solvent-free conditions.[27−37] All these modifications, however, are based on assumptions about a hypothetical reaction mechanism, since very little is known about the mechanism of the Sonogashira reaction, specially for the copper-free variant.

Two different mechanisms have been proposed for the copper-free Sonogashira reaction (Figure 1): the *deprotonation*[19] and *carbopalladation*[38] mechanisms. Both mechanisms share the initial oxidative addition of the organohalide R^1-X to the $PdL_2(0)$ complex giving the intermediate **1** and the subsequent ligand by alkyne substitution from this species, which results in the formation of complex **2**. At this point, the two reaction mechanisms differ in the next steps leading to the final coupled product. More specifically, in the case of the deprotonation mechanism (Figure 1, left) the deprotonation of the alkyne and the coordination of the ligand L take place from **2** yielding a square planar Pd complex with the two organic groups in cis disposition, from which the coupled product is expelled by reductive elimination. Alternatively, in the carbopalladation mechanism (Figure 1, right) complex **2** undergoes addition of the organic group R^1 to the terminal

Received: October 11, 2011
Revised: November 23, 2011
Published: November 29, 2011

   dx.doi.org/10.1021/cs200526x | *ACS Catal.* 2012, 2, 135−144

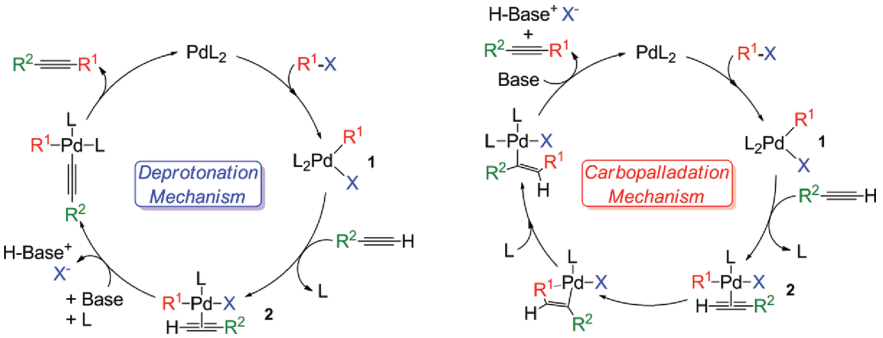

Figure 1. Proposed reaction mechanisms for the copper-free Sonogashira reaction: *deprotonation* (left)[19] and *carbopalladation* (right)[38] mechanisms.

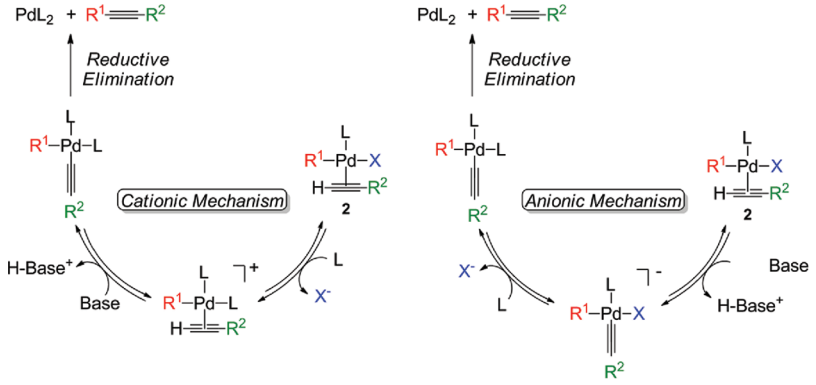

Figure 2. *Cationic* (left) and *anionic* (right) alternatives for the deprotonation mechanism.

Scheme 2. Copper-Free Sonogashira Reaction between Several 4-Substituted Phenylacetylenes and Iodobenzene

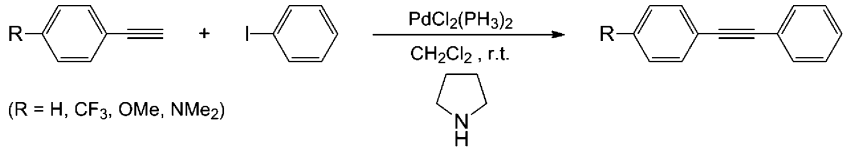

alkyne, followed by the coordination of the ligand L and subsequent base-mediated reductive elimination.

Over the past years, these two mechanisms have been somewhat discussed in the literature, but the mechanism that operates in the copper-free Sonogashira reaction remains still unclear. In fact, up to date, the reported experimental and theoretical mechanistic studies on this process have been rather scarce. Among the experimental ones, one must mention the ones reported by Jutand et al.[39,40] and Mårtensson et al.[41] On one hand, Jutand et al. by means of a thoughtful work shed light on the decelerating effect of alkynes in the oxidative addition step and suggested that amines might have multiple roles in the reaction mechanism. On the other hand, Mårtensson et al.[41] demonstrated with a simple though clever experiment that the carbopalladation mechanism can be discarded, and they proposed two alternative routes for the deprotonation pathway. These two variants of the deprotonation, labeled by the authors as *cationic* and *anionic mechanisms*, only differ in the order of the steps (Figure 2). The cationic mechanism (Figure 2, left) involves the L-X ligand substitution in **2** giving rise to the cationic Pd complex *cis*-$[Pd(R^1)(alkyne)(L)_2]^+$, which undergoes deprotonation of the alkyne by an external base and subsequent reductive elimination. In contrast, in the anionic mechanism (Figure 2, right) the deprotonation of the alkyne occurs first resulting in the anionic complex *cis*-$[Pd(R^1)(acetylide)(X)(L)]^-$, in which the L-X ligand substitution takes place followed by the reductive elimination step. According to Mårtensson et al.,[41] the cationic and the anionic alternatives can be favored depending on the electronic nature of the substituents directly attached to the terminal alkynes. Particularly, the authors suggest that alkynes bearing electron withdrawing groups (EWG) may favor the anionic mechanism whereas alkynes bearing electron donating groups (EDG) may favor the cationic pathway.

As far as the theoretical studies on the reaction mechanism are concerned, to the best of our knowledge, there are those reported by Chen et al.[42] where they considered the halide (Br^-) as the species accepting the proton from the alkyne and by Sikk et al.[43] where a reaction mechanism for the process was analyzed; the latter paper appeared during the revision process of this work. In spite of the importance of the Sonogashira reaction, there is a lack of deep understanding of the reaction mechanism.

The purpose of this work is to evaluate the reaction mechanisms proposed in the literature and possible alternative pathways using a general model of the typical Pd-catalyzed copper-free Sonogashira reaction. To this end, the Gibbs energy profiles of the different mechanistic proposals have been obtained by Density Functional Theory (DFT) calculations. An additional objective of this work is to analyze the effect of the electronic nature of the alkyne's substituents over all the

dx.doi.org/10.1021/cs200526x | *ACS Catal.* 2012, 2, 135–144

studied reaction pathways. This feature for a set of substituents has been investigated by combining theory and experiment.

2. RESULTS AND DISCUSSION

2.1. Selection of the Model. For the analysis of the general reaction mechanism we selected a set of model molecules to obtain a general overview on the process. Hence, phenylacetylene and iodobenzene species were selected as models for the coupling organic reactants, pyrrolidine as base, and dichloromethane (DCM) as solvent. For the additional analysis of the effect of the alkyne's substituents, several 4-substituted phenylacetylenes (R = H, CF_3, OMe, NMe_2) were considered (Scheme 2). As far as the catalyst is concerned, all the calculations were performed using $Pd(PH_3)_2$ as a model for the catalyst. Because of the increase of computational power, this model used to be considered too small, and catalysts with bigger phosphine ligands used to be calculated. Nevertheless, we have selected this model on purpose for this study for the following reasons: (a) as we have recently shown, conformational diversity may introduce significant errors in the calculations of the energy profiles (with modifications in energy barriers higher than 10 kcal·mol^{-1} depending on the phosphines),[44] (b) regarding the electronic properties of the phosphine, PH_3 can be considered as a neutral one, (c) and in terms of computational requirements it is by far the less demanding one. The main objective of the present work is to map the potential energy surface by analyzing all the reasonable reaction profiles. Thus, we think the present model covers most of the general features of the reaction system, apart from the steric effects that should be evaluated for the particular system studied. Full computational details are provided in the Computational Details section.

The oxidative addition of PhI to $[Pd(PH_3)_2]$ is the first step of the reaction giving rise to the *cis*-$[Pd(Ph)(I)(PH_3)_2]$ complex. The calculated energy barrier for this process is rather low, 17.0 kcal·mol^{-1}, as expected for aryl iodides. The subsequent cis-to-trans isomerization is known to take place following different pathways,[45] but in any case it is an easy process.[46] Thus, we focus on analyzing the reaction process starting from the *trans*-$[Pd(Ph)(I)(PH_3)_2]$ (**1**) complex.

2.2. Copper-Free Sonogashira Reaction via a Carbopalladation Mechanism. Despite that Mårtensson et al.[41] experimentally showed that the carbopalladation mechanism can not be operative, to have a comprehensive mechanistic understanding of the reaction we investigated this mechanism together with the deprotonation mechanism including their cationic and anionic alternatives.

The theoretical investigation of the copper-free Sonogashira reaction with phenylacetylene as a model substrate (R = H) through a carbopalladation mechanism afforded the reaction profile shown in Figure 3. As previously mentioned, the carbopalladation and the deprotonation mechanisms share the initial substitution of a phosphine ligand by the alkyne, which leads to the formation of a common intermediate (**2**). The calculation of the associative substitution indicate that this is an endergonic process by 13.5 kcal·mol^{-1} with an energy barrier of 23.0 kcal·mol^{-1}. Once complex **2** is formed, the carbopalladation reaction occurs through the transition state **C-TS1** resulting in the intermediate **C-1** with a relative energy barrier of 14.2 kcal·mol^{-1}. Subsequently, this intermediate evolves with a low energy barrier (6.4 kcal·mol^{-1}) to the very stable intermediate **C-2** (Figure 4) by coordination of a phosphine ligand via **C-TS2**. Finally, the alkenyl moiety in **C-2** is

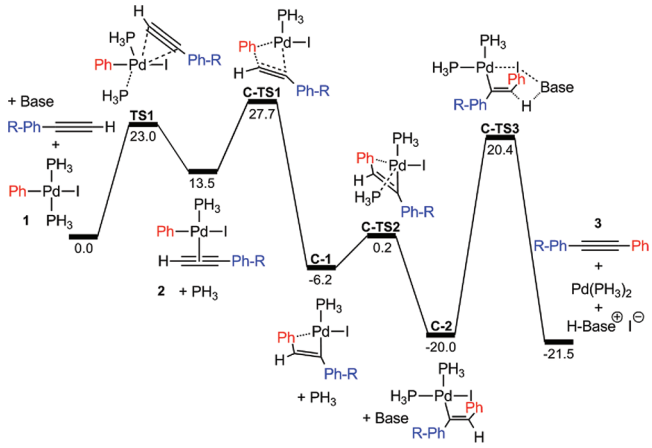

Figure 3. Gibbs energy profile in DCM (ΔG_{DCM}, kcal·mol^{-1}) at 298 K for the carbopalladation mechanism with R = H, and Base = pyrrolidine.

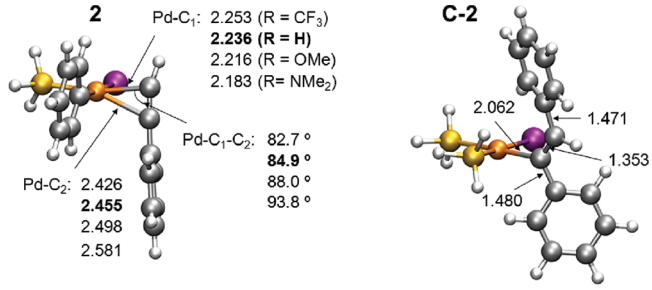

Figure 4. Optimized structures for intermediates **2** and **C-2** with phenylacetylene (R = H). Distances (shown in Å) and angles in complex **2** with the other R groups are also shown.

deprotonated by an external base through the transition state **C-TS3** yielding the final coupled product (**3**) and the regeneration of the catalyst. This last step has the highest energy barrier in the overall energy profile (40.4 kcal·mol^{-1}), which can be attributed to the high stability of **C-2** and the difficulty that the deprotonation of a double bond entails (high energy of **C-TS3**). As a result, this step has the highest energy barrier in the carbopalladation mechanism with phenylacetylene (R = H).

Overall, the reaction is exergonic by 21.5 kcal·mol^{-1}, but the carbopalladation mechanism has a very high energy barrier (40.4 kcal·mol^{-1}), making it unfeasible for the copper-free Sonogashira reaction. The occurrence of a very stable intermediate placed 20 kcal·mol^{-1} below reactants and the necessity of overcoming a barrier of about 40 kcal·mol^{-1} are responsible for the unsuitability of the carbopalladation mechanism. This theoretical finding agrees with the experimental observation of Mårtensson et al.[41] that a complex analogue to **C-2** synthesized through an alternative route does not afford the coupled product under the Sonogashira reaction conditions.

As far as the effect of the electronic nature of the R substituents of the alkyne is concerned, the Gibbs energy profiles for the Sonogashira reaction with several 4-substituted phenylacetylenes (R = CF_3, OMe, NMe_2) through a carbopalladation mechanism were also computed (Table 1).

As shown in Table 1, the influence of the substituent on the reaction energy is rather low: the reaction is highly exergonic with all the substituents by around 21 kcal·mol^{-1}. The most

dx.doi.org/10.1021/cs200526x | ACS Catal. 2012, 2, 135–144

Table 1. Relative Gibbs Energies in DCM (ΔG_{DCM}, kcal·mol^{-1}) at 298 K for the Carbopalladation Mechanism with the Different 4-Substituted Phenylacetylenes (R = H, CF_3, OMe, NMe_2)

species	R = H	R = CF_3	R = OMe	R = NMe_2
1 + Base + alkyne	0.0	0.0	0.0	0.0
TS1	23.0	24.8	22.9	20.6
2 + PH_3	13.5	15.9	12.7	9.9
C-TS1	27.7	28.3	27.5	26.7
C-1	−6.2	−7.1	−5.7	−5.4
C-TS2	0.2	−1.8	0.2	−0.1
C-2	−20.0	−21.5	−19.5	−19.8
C-TS3	20.4	19.4	21.3	21.2
3 + [$Pd(PH_3)_2$] + H-Base$^+$ I^-	−21.5	−21.6	−21.3	−21.4

important effect of the different R groups is in the step common to all the mechanisms, which is the coordination of the alkyne to the palladium complex **1** to yield complex **2**. However, this is not the rate-determining step in the carbopalladation mechanism. The calculated energy barrier for this step (Table 1, **TS1**) decreases in the order: R = CF_3 > H > OMe > NMe_2, which correlates with the higher electron donor ability of the R groups, and consequently, with the higher donor ability of the alkyne. This higher donor ability of the alkyne with EDGs is responsible for the higher stability of the corresponding complexes **2**, which feature shorter Pd−C_1 distances and higher Pd−C_1−C_2 angles with these substituents (Figure 4).

Similarly to the case with R = H, the deprotonation of the alkene moiety in **C-2** with the other R groups has the highest energy barrier in the overall reaction pathway, with values ranging from 40.4 to 41.0 kcal·mol^{-1} (Table 1). Thus, for these substituted phenylacetylenes the carbopalladation mechanism is also too energy-demanding to be operative under the reaction conditions, which agrees again with the experimental findings of Mårtensson et al.[41]

2.3. Copper-Free Sonogashira Reaction via a Deprotonation Mechanism. The copper-free Sonogashira reaction through a deprotonation mechanism was also investigated. As mentioned in the introduction, for this mechanism two different alternatives have been proposed, namely the *cationic* and the *anionic* mechanisms (Figure 2).[41]

2.3.1. Copper-Free Sonogashira Reaction via a Cationic Mechanism. The cationic mechanism differs from the anionic mechanism by the order in which the deprotonation and substitution steps occur (Figure 2). The computed Gibbs energy profile for the copper-free Sonogashira reaction with phenylacetylene (R = H) through a cationic mechanism is shown in Figure 5. In contrast to the carbopalladation mechanism, once complex **2** is formed, the substitution of the iodide by the phosphine ligand takes place giving rise to the ion-pair (**DC-1**) formed between the cationic Pd complex and the iodide with a relative energy barrier of 14.0 kcal·mol^{-1} (**DC-TS1**). Then, from this species the deprotonation of the alkyne by the external base occurs (**DC-TS2**, 25.9 kcal·mol^{-1}) yielding the intermediate **RE-1**, where the two organic groups are in a cis configuration. Finally, **RE-1** undergoes reductive elimination via **RE-TS1** (17.9 kcal·mol^{-1}) resulting in the final product (**3**) and the regeneration of the catalyst. In the overall energy profile, the highest global energy barrier corresponds to the iodide-by-phosphine ligand substitution via **DC-TS1** (27.5 kcal·mol^{-1}).

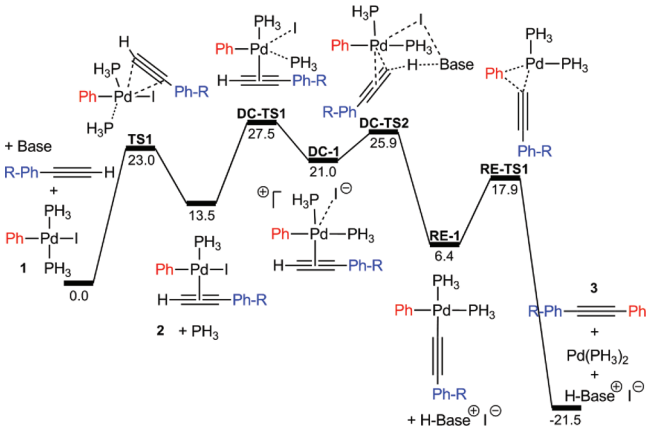

Figure 5. Gibbs energy profile in DCM (ΔG_{DCM}, kcal·mol^{-1}) at 298 K for the cationic mechanism with R = H, and Base = pyrrolidine.

The Gibbs energy profiles for the Sonogashira reaction via the cationic mechanism with the other 4-substituted phenylacetylenes (R = CF_3, OMe, NMe_2) were also computed (Table 2). Interestingly, the energy of the transition state for the substitution of the iodide by the phosphine ligand (the energy difference between **DC-TS1** and **1**) with the different R groups increases in the order R = NMe_2 < OMe < H < CF_3. However, the relative energy barrier for this step (the energy difference between **DC-TS1** and **2**) is practically the same for all the R groups (the highest energy difference between the R groups is 0.8 kcal·mol^{-1}), which indicates that the different stability of intermediates **2** is responsible for the differences in the global energy barriers. On the other hand, Table 2 shows that the deprotonation of the alkyne in **DC-1** through **DC-TS2** follows a similar trend as the iodide-for-phosphine substitution step (NMe_2 < OMe < CF_3 < H). In this case, however, the overall energy barrier range (the energy differences between **DC-TS2** and **DC-1**) is slightly higher (the lowest energy difference between the R groups is 1.4 kcal·mol^{-1}). More specifically, the relative energy barriers for the deprotonation step increase in the following order: CF_3 < OMe ≈ H < NMe_2. This trend can be rationalized: the presence of a EWG (i.e., R = CF_3) in the alkyne makes its proton more acidic and thus, the relative energy barrier for this step decreases. Conversely, the presence of an EDG (i.e., R = NMe_2) makes the proton of the alkyne less acidic, which increases the relative energy barrier. The cases with the model substituent (i.e., R = H) and the moderate EDG

Table 2. Relative Gibbs Energies in DCM (ΔG_{DCM}, kcal·mol^{-1}) at 298 K for the Cationic Mechanism with the Different 4-Substituted Phenylacetylenes (R = H, CF_3, OMe, NMe_2)

species	R = H	R = CF_3	R = OMe	R = NMe_2
1 + Base + alkyne	0.0	0.0	0.0	0.0
TS1	23.0	24.8	22.9	20.6
2 + PH_3	13.5	15.9	12.7	9.9
DC-TS1	27.5	29.1	26.4	23.7
DC-1	21.0	22.2	20.6	16.1
DC-TS2	25.9	25.5	25.3	21.5
RE-1	6.4	4.3	7.1	6.8
RE-TS1	17.9	15.5	18.8	18.8
3 + [$Pd(PH_3)_2$] + H-Base$^+$ I^-	−21.5	−21.6	−21.3	−21.4

dx.doi.org/10.1021/cs200526x | *ACS Catal.* 2012, 2, 135−144

(i.e., R = OMe) have similar energy barriers and lie in between the other R groups.

Similarly to the reaction with phenylacetylene (R = H), the highest energy point in the overall energy profile regardless of the R groups corresponds to the substitution of the iodide by the phosphine ligand (**DC-TS1**); therefore this step has also the highest energy barrier for all these R groups. Moreover, these calculated energy barriers are lower for EDGs than for EWGs indicating that the more EDG the faster the process via this cationic mechanism should be.

2.3.2. Copper-free Sonogashira Reaction via an Anionic Mechanism. In the anionic mechanism the steps of the deprotonation mechanism take place in reverse order compared to the cationic mechanism. Thus, in the anionic mechanism the deprotonation of the alkyne by the external base from complex **2** occurs first, followed by the iodide-for-phosphine substitution. The Gibbs energy profile of the Sonogashira reaction with phenylacetylene (R = H) through the anionic mechanism is shown in Figure 6.

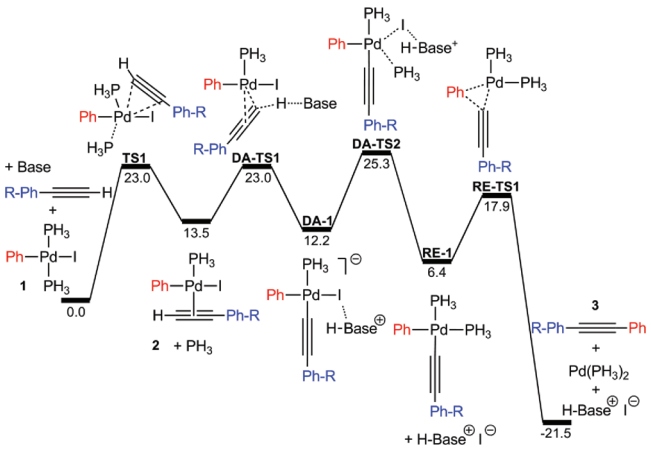

Figure 6. Gibbs energy profile in DCM (ΔG_{DCM}, kcal·mol^{-1}) at 298 K for the anionic mechanism with R = H, and Base = pyrrolidine.

The deprotonation of the alkyne by the external base in complex **2** occurs through the transition state **DA-TS1** (23.0 kcal·mol^{-1}) and leads to the formation of the ion-pair (**DA-1**) formed between the anionic Pd complex and the protonated base. Subsequently, this species evolves to intermediate **RE-1** by an iodide-by-phosphine substitution via **DA-TS2**. This step corresponds to the highest transition state within the energy profile (2.3 kcal·mol^{-1} higher than **DA-TS1** and **TS1**). Finally, **RE-1** undergoes reductive elimination giving rise to the coupling product and regenerating the catalyst.

The relative Gibbs energy values for the other 4-substituted phenylacetylenes (R = CF_3, OMe, NMe_2) were also computed and are summarized in Table 3. For all the 4-substituted phenylacetylenes, Table 3 shows that the highest energy barrier corresponds to the substitution of the iodide by the phosphine ligand via **DA-TS2**, indicating that this step, like with R = H, is rate limiting in the anionic mechanism. Moreover, the small energy differences between the transition states **DA-TS2** (all of them within 1 kcal·mol^{-1}) suggest that the electronic nature of the R groups may not have a significant effect over the reaction rates through this mechanism.

2.3.3. Cationic Mechanism versus Anionic Mechanism. According to calculations, in both cationic and anionic mechanisms the highest energy barrier corresponds to the

Table 3. Relative Gibbs Energies in DCM (ΔG_{DCM}, kcal·mol^{-1}) at 298 K for the Anionic Mechanism with the Different 4-Substituted Phenylacetylenes (R = H, CF_3, OMe, NMe_2)

species	R = H	R = CF_3	R = OMe	R = NMe_2
1 + Base + alkyne	0.0	0.0	0.0	0.0
TS1	23.0	24.8	22.9	20.6
2 + PH_3	13.5	15.9	12.7	9.9
DA-TS1	23.0	23.1	22.3	19.3
DA-1	12.2	10.8	12.3	12.5
DA-TS2	25.3	24.6	25.8	25.6
RE-1	6.4	4.3	7.1	6.8
RE-TS1	17.9	15.5	18.8	18.8
3 + $[Pd(PH_3)_2]$ + H-Base$^+$ I$^-$	−21.5	−21.6	−21.3	−21.4

substitution of the iodide by the phosphine ligand. However, depending on the mechanism this substitution takes place either before (i.e., the cationic mechanism) or after (i.e., the anionic mechanism) the deprotonation of the alkyne. More specifically, in the case of the cationic mechanism this substitution takes place in complex **2** via **DC-TS1** (Figure 5), whereas in the anionic mechanism it occurs in **DA-1** via **DA-TS2** (Figure 6). The computed global Gibbs energy barriers for these processes with all the 4-substituted phenylacetylenes (Table 4) show that both mechanisms are feasible. Importantly,

Table 4. Global Gibbs Energy Barriers in DCM (ΔG_{DCM}, kcal·mol^{-1}) at 298 K for the Cationic and Anionic Mechanisms with the Different 4-Substituted Phenylacetylenes (R = H, CF_3, OMe, NMe_2)

	global Gibbs energy barriers[a]	
substituent	cationic mechanism	anionic mechanism
R = CF_3	29.1	**24.6**
R = H	27.5	**25.3**
R = OMe	26.4	**25.8**
R = NMe_2	**23.7**	25.6

[a]The Gibbs energy barriers for the lowest-energy deprotonation pathways with the different R groups are in bold.

these values also suggest that depending on the electronic nature of the R group there might be a change in the reaction mechanism. In particular, with both the highly electron withdrawing group R = CF_3 and the model substituent R = H, the anionic mechanism is favored compared to the cationic mechanism by 4.5 and 2.2 kcal·mol^{-1}, respectively. On the other hand, with the moderate electron donating group R = OMe this energy difference becomes smaller (0.6 kcal·mol^{-1}) but still in favor of the anionic mechanism. Finally, with the highly electron donating group R = NMe_2 this energy difference is reversed favoring the cationic mechanism by 1.9 kcal·mol^{-1}.

This predicted change in the reaction mechanism can be rationalized as follows: the first step in the cationic mechanism yields intermediate **2** (Figure 5). As previously stated, in the case of EWGs (i.e., R = CF_3, H) or moderate EDGs (i.e., R = OMe) this species is less stable than with highly EDGs (i.e., R = NMe_2) (the energy difference range from 2.8 kcal·mol^{-1} to 6.0 kcal·mol^{-1}). Thus, EWGs groups cause higher energy barriers because the following iodide-by-phosphine substitution step has a very similar relative energy barrier for all the R groups. In contrast, the first step in the anionic mechanism from complex

dx.doi.org/10.1021/cs200526x | ACS Catal. 2012, 2, 135−144

2 gives the intermediate **DA-1** (Figure 6). In this case, the anionic charge on the Pd complex is better stabilized with EWGs, which offsets the energy gain in complex **2** with the highly EDGs and leads to lower energy barriers compared to the cationic mechanism. This results in a preference for the anionic mechanism with EWGs (i.e., R = CF_3, H) or moderate EDGs (i.e., R = OMe) and a preference for the cationic mechanism with highly EDGs (i.e., R = NMe_2).

2.4. Alternative Mechanism: The Ionic Mechanism. Recently, some of us reported a combined experimental and theoretical study on the transmetalation step in a Negishi cross-coupling reaction[47] in which we demonstrated that an external coordinating ligand (i.e., $PMePh_2$, THF) can easily replace the chloride from the complex *trans*-[$PdMeCl(PMePh_2)_2$] (complex analogue to **1**). The reaction mechanism involving this step was labeled as *ionic mechanism*. The role of additional ligands has been also shown to be important in related Sonogashira processes.[48,49] On the basis of these results and that the coordination of the alkyne requires a considerably high energy barrier (higher than 20 kcal·mol^{-1}), we computed an alternative mechanism for the Sonogashira reaction that we also named *ionic mechanism* because of its similarities with the one reported for the Negishi coupling.[47] The computed Gibbs energy reaction profile via this mechanism with phenylacetylene (R = H) is shown in Figure 7.

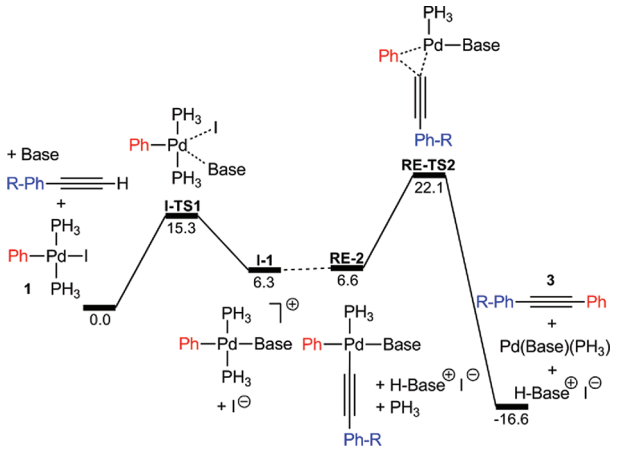

Figure 7. Gibbs energy profile in DCM (ΔG_{DCM}, kcal·mol^{-1}) at 298 K for the ionic mechanism with R = H, and Base = pyrrolidine.

In contrast to the cationic and anionic mechanisms, where the iodide is always expelled after the coordination of the alkyne, in the ionic mechanism it is replaced by the base in the first step. This process occurs through the transition state **I-TS1** and results in the formation of the cationic Pd complex **I-1**. Importantly, the energy barrier required for this process is 15.3 kcal·mol^{-1}, which is much lower (it is at least 5 kcal·mol^{-1} lower) than the energy required for the coordination of the alkyne to **1** via **TS1**. At this point, and on the basis that the reaction is carried out with an excess of base, we considered that the corresponding phenylacetylide may be present in solution as a result of the acid–base reaction. According to calculations, the phenylacetylide can replace one of the phosphine ligands in **I-1** with a barrierless process.[50] This process without energy barrier affords the isoenergetic species **RE-2**, which directly evolves to the desired alkyne (**3**) by common reductive elimination via **RE-TS2** (22.1 kcal·mol^{-1}).[51−54] The relative Gibbs energies for the reactions with the other 4-substituted phenylacetylenes through this ionic mechanism are collected in Table 5.

Table 5. Relative Gibbs Energies in DCM (ΔG_{DCM}, kcal·mol^{-1}) at 298 K for the Ionic Mechanism with the Different 4-Substituted Phenylacetylenes (R = H, CF_3, OMe, NMe_2)

species	R = H	R = CF_3	R = OMe	R = NMe_2
1 + Base + alkyne	0.0	0.0	0.0	0.0
I-TS1	15.3	15.3	15.3	15.3
I-1	6.3	6.3	6.3	6.3
RE-2	6.6	3.5	6.0	6.4
RE-TS2	22.1	18.5	22.6	21.8
3 + [Pd(base)(PH_3)] + H-Base$^+$ I$^-$	−16.6	−16.7	−16.4	−16.5

As shown in Table 5, the highest energy barrier corresponds to the reductive elimination step from complex **RE-2**. The calculated energy barriers for this process with the different R groups range from 18.5 (R = CF_3) to 22.6 kcal·mol^{-1} (R = OMe), which indicates that this ionic mechanism might be competitive with the cationic and anionic mechanisms. Interestingly, the reaction rate through this ionic mechanism depends on the concentration of acetylide present in solution, which is also directly linked to the concentration of the base. In other words, this mechanism depends on the base[55] and the acidity of the proton of the alkyne, which at the same time depends on the electron withdrawing ability of the R group coordinated to the alkyne. Thus, the reaction through this mechanism is expected to be faster when alkynes bearing EWGs are used.

2.5. Effect of the R Substituents on R-C_6H_4–C≡C–H from Experiments. Theoretical calculations demonstrate that the carbopalladation mechanism is not operating under the reaction conditions. Furthermore, calculations also show that the other three investigated mechanisms (i.e., cationic, anionic, and ionic mechanisms) may have competitive rates. Thus, a change on the reaction conditions (i.e., solvent, ligands, substrates, base, etc.) might favor one or another mechanism.

Regarding the effect of the R groups, the theoretical results show relatively small energy differences in the activation energies for the Sonogashira reactions with the different 4-substituted phenylacetylenes (Tables 4 and 5). At this point, we decided to carry out experimental copper-free Sonogashira reactions of 1-fluoro-4-iodobenzene with the 4-substituted phenylacetylenes used for the computational study for comparison. These couplings were performed in dichloromethane with $PdCl_2(PPh_3)_2$ (2 mol %) as catalyst and pyrrolidine as base at room temperature and under Ar atmosphere. In these reactions, the values of conversion (%) of the desired alkyne **3** versus time were obtained by monitoring the reactions by ^{19}F NMR spectroscopy (Figure 8).

The conversion/time data plotted in Figure 8 show that the reaction rate increases with the electron withdrawing ability of the R group (R = NMe_2 < OMe < H ≈ CF_3). Thus, according to experiments, the more acidic the proton of the alkyne is, the higher the reaction rate is; this experimental trend is supported by the ionic mechanism. Notice that if we compare the ratio of conversion of **3** after 1 h for the fastest (R = CF_3) and the slowest (R = NMe_2) reaction, it is 5:1.[56] In terms of activation energies this ratio corresponds to an energy difference lower

dx.doi.org/10.1021/cs200526x | ACS Catal. 2012, 2, 135−144

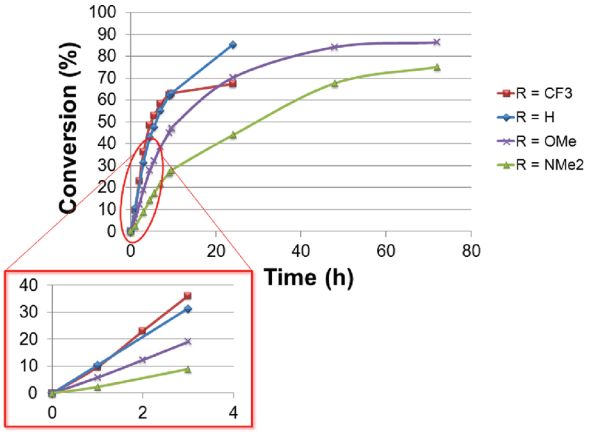

Figure 8. Conversion/time data, obtained by ^{19}F NMR, for the Sonogashira reaction with the analyzed 4-substituted phenylacetylenes (R = H, CF_3, OMe, NMe_2).

than 1 kcal·mol^{-1}, which means that the activation energies for the different R groups are very similar, in agreement with theoretical calculations. According to these results there is not a clear preference for either the deprotonation or the ionic mechanism. Thus, the precise mechanism for a coupling reaction need to be evaluated in detail for each particular case, and competitive mechanisms may take place together. The analysis on a model system for the Suzuki cross-coupling reaction gave rise to similar conclusions regarding the operative reaction mechanism.[45]

3. CONCLUSIONS

The reaction mechanism for the copper-free Sonogashira reaction between iodobenzene and several 4-substituted phenylacetylenes (R = H, CF_3, OMe, NMe_2) was investigated. To the best of our knowledge, this is the first theoretical study that investigates all the reported mechanistic proposals for the copper-free Sonogashira reaction. The theoretical results show that the carbopalladation mechanism has a very high energy barrier, which indicates that this mechanism is not operating under the reaction conditions. For the proposed cationic and the anionic alternatives in the deprotonation mechanism,[41] the calculated Gibbs energy barriers indicate that both mechanisms are feasible. Moreover, calculations predict that one or the other reaction mechanism is favored depending on the electronic nature of the R group coordinated to the alkyne. Thus, EWGs (R = CF_3, H) or moderate EDGs (R = OMe) might favor an anionic mechanism, whereas highly EDGs (R = NMe_2) might favor a cationic mechanism. These differences can be attributed to the different stability of the intermediates that precede the highest energy barrier; the relative intermediate stabilities depend on the R group. These results are in agreement with the reported experimental work of Mårtensson et al.[41]

The presence of an excess of a coordinating ligand like pyrrolidine, the base, and the presence of phenylacetylide opens a new reaction pathway for the copper-free Sonogashira reaction: the ionic mechanism. In this mechanism the base substitutes the halide and helps in forming acetylide species. The theoretical results for this mechanism show that it is competitive with the analyzed cationic and anionic mechanisms and that it may lead to higher reaction rates with alkynes bearing EWGs, which agrees with experiments. Overall, these results suggest that in the copper-free Sonogashira reaction, like in other cross-coupling reactions (i.e., Stille, Negishi), there are several reaction pathways that may have competitive rates, and a change on the reaction conditions (i.e., solvent, ligands, substrates, base, etc.) might favor one over the other reaction mechanisms. Thus, a detailed study of a specific reaction is required to assess which mechanism is favored on a particular system. The present study on a general model of Pd-catalyzed copper-free Sonogashira reaction has mapped out the reaction scenario, and shows the complexity of this process.

4. COMPUTATIONAL DETAILS

All calculations were performed at DFT level by means of the hybrid Becke3LYP[57,58] functional as implemented in Gaussian03 program package.[59] Pd and I atoms were described using the Stuttgart-Dresden (SDD) effective core potential[60] for the inner electrons and its associated double-ζ basis set for the outer ones. Additionally, for these atoms f-polarization (exponent 1.472)[61] and d-polarization (exponent 0.289)[62] shells were added, respectively. In the case of I atoms diffuse functions were also added (exponent 0.0308).[63] For the C, P, H atoms and the N atoms the 6-31G(d,p) and the 6-31+g(d) basis sets were used, respectively. Such a computational level has been widely employed in theoretical studies on related cross-coupling reactions providing good results.[46,64−69] The structures of the reactants, intermediates, and transition states were fully optimized without any symmetry constraint. During these optimizations, no artifactual interactions involving hydrogens of the PH_3 model phosphine were detected. Harmonic force constants were computed at the optimized geometries to characterize the stationary points as minima or saddle points. The latter were confirmed by having one imaginary frequency in the Hessian matrix and correlating the corresponding reactants and products. The entropic contributions were evaluated at a pressure of 382 atm to model the changes in entropy for a condensed phase.[70,71] Solvent effects (CH_2Cl_2, ε = 8.930) were introduced through single point calculations at optimized gas-phase geometries for all the minima and transition states by means of a continuum method, the PCM approach[72] implemented in Gaussian03. Moreover, the default cavity model was modified by adding individual spheres to the hydrogen atoms directly linked to the alkyne and to the nitrogen atom of the pyrrolidine molecule, using the keyword SPHEREONH. The relative Gibbs energies in dichloromethane shown throughout this present work (ΔG_{DCM}) were obtained by employing the following scheme: $\Delta G_{DCM} = \Delta E_{DCM} + (\Delta G_{gas} - \Delta E_{gas})$.

5. EXPERIMENTAL DETAILS

General Procedures. All the reagents and dry solvents were obtained from commercial sources. Flash chromatography was performed on silica gel 60 (0.040−0.063 mm). Thin layer chromatography was performed on precoated silica gel plates and the spots were visualized under UV light (λ = 254 nm). Mp were determined on a hot stage apparatus. Gas chromatographic analyses were performed on an instrument equipped with a fused silica capillary column. IR data (only the structurally most important peaks are listed) were collected on a FT spectrophotometer in cm^{-1}. ^1H NMR spectra were recorded at 300 MHz. Chemical shifts are reported in ppm using tetramethylsilane (TMS, 0.00 ppm) as internal standard. ^{13}C NMR spectra were recorded at 75 MHz. ^{19}F NMR spectra

dx.doi.org/10.1021/cs200526x | ACS Catal. 2012, 2, 135−144

were recorded at 282.1 MHz with $CFCl_3$ as the internal reference. Low-resolution electron impact (EI) mass spectra were obtained on a GC-MS spectrometer at 70 eV. High resolution mass spectra were performed at the MS service of the University of Alicante. Solid products were recrystallized in hexane/Et_2O unless otherwise stated, and melting points were not corrected. All reactions were carried out under an argon atmosphere in dried glassware. The products 1-fluoro-4-(phenylethynyl)benzene (**3a**), 1-fluoro-4-{[4-(trifluoromethyl)-phenyl]ethynyl}benzene (**3b**), and 1-fluoro-4-[(4-methoxyphenyl)ethynyl]benzene (**3c**) have been previously reported.

Preparation of Alkynes 3. To a stirred solution of $PdCl_2(PPh_3)_2$ (7.0 mg, 0.01 mmol, 2 mol % Pd) in dry CH_2Cl_2 (1 mL, 0.5 M) was added 1-fluoro-4-iodobenzene (58 μL, 0.5 mmol), alkyne (0.55 mmol), and pyrrolidine (84 μL, 1 mmol) at room temperature under an argon atmosphere. Stirring was continued at room temperature for 10−30 h. The reaction mixture was then quenched with H_2O (4 mL). The mixture was extracted with EtOAc (3 × 6 mL). The organic layer was dried over $MgSO_4$, followed by removal of the solvent at reduced pressure. The resulting crude was purified by silica gel column chromatography.

1-Fluoro-4-(phenylethynyl)benzene (3a).[73]

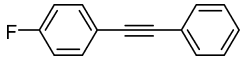

Pale yellow solid; mp 109−111 °C (Lit. 108−109 °C); ^{1}H NMR ($CDCl_3$) δ 7.00−7.06 (m, 2H), 7.30−7.37 (m, 3H), 7.47−7.54 (m, 4H); ^{13}C NMR ($CDCl_3$) δ 82.3, 89.0, 115.6 (d, J = 21.9 Hz), 119.3 (d, J = 3.4 Hz), 123.1, 128.30, 128.34, 131.5, 133.4 (d, J = 8.3 Hz), 162.5 (d, J = 247.9 Hz); ^{19}F NMR (282.1 MHz, $CDCl_3$) δ −111.5; IR (ν, cm^{-1}) 1594, 1509 (Ar); MS (GC-MS, EI): m/z 196 (M, 100%), 194 (M-2, 13%).

1-Fluoro-4-{[4-(trifluoromethyl)phenyl]ethynyl]}-benzene (3b).[74]

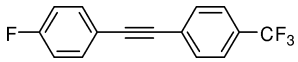

Colorless solid; mp 75−77 °C; ^{1}H NMR (300 MHz, $CDCl_3$) δ 7.01−7.09 (m, 2H), 7.48−7.55 (m, 2H), 7.59 (bs, 4H); ^{13}C NMR (75 MHz, $CDCl_3$) δ 87.7, 90.6, 115.8 (d, J = 22.1 Hz), 118.7 (d, J = 3.4 Hz), 123.9 (q, J = 270.3 Hz), 125.3 (q, J = 3.6 Hz), 126.9, 130.0 (q, J = 32.5 Hz), 131.7, 133.7 (d, J = 8.4 Hz), 162.8 (d, J = 248.9 Hz); ^{19}F NMR (282.1 MHz, $CDCl_3$) δ −110.4, −63.3; IR (ν, cm^{-1}) 2223 (C≡C), 1597, 1501 (Ar); MS (GC-MS, EI): m/z 264 (M, 100%), 263 (M-1, 16%), 245 (M-19, 11%).

1-Fluoro-4-[(4-methoxyphenyl)ethynyl]benzene (3c).[75]

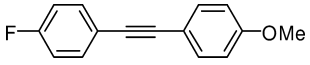

Pale yellow solid {it is a mixture 9:1 of desired product and diyne [1,4-bis(4-methoxyphenyl)buta-1,3-diyne]}; mp 90−92 °C (mixture); ^{1}H NMR (300 MHz, $CDCl_3$) δ 3.80 (s, 3H), 6.82−6.89 (m, 2H), 6.98−7.05 (m, 2H), 7.43−7.50 (m, 4H); ^{13}C NMR (75 MHz, $CDCl_3$) δ 55.2, 86.9, 89.0, 114.0, 115.1, 115.5 (d, J = 21.9 Hz), 119.6 (d, J = 3.5 Hz), 133.0, 133.2 (d, J = 8.2 Hz), 159.6, 162.2 (d, J = 247.4 Hz); ^{19}F NMR (282.1 MHz, $CDCl_3$) δ −112.1; IR (ν, cm^{-1}) 2838, 2217 (C≡C), 1903, 1596, 1509 (Ar); MS (GC-MS, EI): m/z 226 (M, 100%), 211 (M-15, 49%), 183 (36).

4-[(4-Fluorophenyl)ethynyl]-*N*,*N*-dimethylaniline (3d).

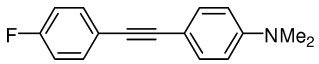

Pale brown solid; mp 135−137 °C; ^{1}H NMR (300 MHz, $CDCl_3$) δ 2.96 (bs, 6H), 6.58−6.69 (m, 2H), 6.96−7.04 (m, 2H), 7.35−7.50 (m, 4H); ^{13}C NMR (75 MHz, $CDCl_3$) δ 40.1, 86.2, 90.2, 109.7, 111.8, 115.4 (d, J = 21.8 Hz), 120.2 (d, J = 3.4 Hz), 132.6, 133.0 (d, J = 8.1 Hz), 150.1, 162.0 (d, J = 246.7 Hz); ^{19}F NMR (282.1 MHz, $CDCl_3$) δ −112.8; IR (ν, cm^{-1}) 2210 (C≡C), 1609, 1500 (Ar); MS (GC-MS, EI): m/z 240 (M+1, 17%), 239 (M, 100%), 238 (M−1, 56%), 223 (17), 194 (10), 119 (13); HRMS (ESI): m/z 239.1131, calcd. for $C_{16}H_{14}FN$: 239.1110.

Kinetics of the Copper-Free Sonogashira Reaction. ^{19}F NMR Decoupled Studies. To a solution of $PdCl_2(PPh_3)_2$ (7.0 mg, 0.01 mmol, 2 mol % Pd) in $CDCl_3$ (3 mL) was added a solution of 1-fluoro-4-iodobenzene (58 μL, 0.5 mmol), alkyne (0.5 mmol), and pyrrolidine (251 μL, 3 mmol) in $CDCl_3$ (2 mL) at room temperature under an argon atmosphere. The reaction mixture was stirred mechanically for 30 s. After 10 min, an aliquot of 0.7 mL was removed, and the reaction process was monitored by ^{19}F NMR decoupled studies.

■ ASSOCIATED CONTENT

Ⓢ Supporting Information

Cartesian coordinates and absolute energies for all computed structures and spectra and kinetic data of the synthesized alkynes **3**. This material is available free of charge via the Internet at http://pubs.acs.org.

■ AUTHOR INFORMATION

Corresponding Author

*E-mail: cnajera@ua.es (C.N.), agusti@klingon.uab.es (A.L.), gregori@klingon.uab.es (G.U.).

Funding

We thank the Ministerio de Ciencia e Innovación (MICINN) (Projects FEDER-CTQ2007-62771/BQU, CTQ2008-06866-C02-01, CTQ2010-20387, CTQ2011-23336 and ORFEO Consolider Ingenio 2010 CSD2007-00006), the Generalitat Valenciana (PROMETEO/2009/038), the Generalitat de Catalunya (2009/SGR/68), and the University of Alicante for financial support, and the Universitat Autònoma de Barcelona for the scholarship to M.G.-M. (UAB PIF). M.P. thanks the MICINN for financial support under the JdC program. We are also grateful to CESCA for generous allocation of computer time.

■ REFERENCES

(1) For reviews, see: Sonogashira, K. *J. Organomet. Chem.* **2002**, *653*, 46 , and refs 2−6.
(2) Negishi, E.-I.; Anastasia, L. *Chem. Rev.* **2003**, *103*, 1979.
(3) Tykwinski, R. R. *Angew. Chem., Int. Ed.* **2003**, *42*, 1566.
(4) Chinchilla, R.; Nájera, C. *Chem. Rev.* **2007**, *107*, 874.
(5) Chinchilla, R.; Nájera, C. *Chem. Soc. Rev.* **2011**, *40*, 5084.
(6) Bunz, U. H. F. *Chem. Rev.* **2000**, *100*, 1605.
(7) Nicolaou, K. C.; Bulger, P. G.; Sarlah, D. *Angew. Chem., Int. Ed.* **2005**, *44*, 4442.
(8) Müller, T. J. J.; D'Souza, D. M. *Pure Appl. Chem.* **2008**, *80*, 609.

(9) Shiedel, M.-S.; Briehn, C. A.; Bäuerle, P. *J. Organomet. Chem.* **2002**, *653*, 200.
(10) Hortholary, C.; Coudret, C. *J. Org. Chem.* **2003**, *68*, 2167.
(11) Zapf, A.; Beller, M. *Top. Catal.* **2002**, *19*, 101.
(12) Torborg, C.; Beller, M. *Adv. Synth. Catal.* **2009**, *351*, 3027.
(13) Sonogashira, K.; Tohda, Y.; Hagihara, N. *Tetrahedron Lett.* **1975**, *16*, 4467.
(14) Ljungdahl, T.; Pettersson, K.; Albinsson, B.; Mårtensson, J. *J. Org. Chem.* **2006**, *71*, 1677.
(15) Gelman, D.; Buchwald, S. L. *Angew. Chem., Int. Ed.* **2003**, *42*, 5993.
(16) Kotora, M.; Takahashi, T. In *Handbook of Organopalladium Chemistry for Organic Synthesis*; Negishi, E.-I., de Meijere, A., Eds.; Wiley-Interscience: New York, 2002; p 973.
(17) Siemsen, P.; Livingston, R. C.; Diederich, F. *Angew. Chem., Int. Ed.* **2000**, *39*, 2632.
(18) For selected papers on Pd-catalyzed Sonogashira reactions under Cu-free conditions, see: Fukuyama, T.; Shinmen, M.; Nishitani, S.; Sato, M.; Ryu, I. *Org. Lett.* **2002**, *4*, 1691 , and refs 19−26.
(19) Soheili, A.; Albaneze-Walker, J.; Murry, J. A.; Dormer, P. G.; Hughes, D. L. *Org. Lett.* **2003**, *5*, 4191.
(20) Nájera, C.; Gil-Moltó, J.; Karlström, S.; Falvello, L. R. *Org. Lett.* **2003**, *5*, 1451.
(21) Rau, S.; Lamm, K.; Görls, H.; Schöffel, J.; Walther, D. *J. Organomet. Chem.* **2004**, *689*, 3582.
(22) Li, J.-H.; Zhang, X.-D.; Xie, Y.-X. *Eur. J. Org. Chem.* **2005**, 4256.
(23) Gil-Moltó, J.; Nájera, C. *Eur. J. Org. Chem.* **2005**, 4073.
(24) Yi, C.; Hua, R. *Catal. Commun.* **2006**, *7*, 377.
(25) Galdino de Lima, P.; Antunes, O. A. C. *Tetrahedron Lett.* **2008**, *49*, 2506.
(26) Komáromi, A.; Tolnai, G. L.; Novák, Z. *Tetrahedron Lett.* **2008**, *49*, 7294.
(27) For selected papers on Sonogashira reactions under both Cu-free and amine-free conditions, see: Alonso, D. A.; Nájera, C.; Pacheco, M. C. *Tetrahedron Lett.* **2002**, *43*, 9365 , and refs 28−32.
(28) Cheng, J.; Sun, Y.; Wang, F.; Guo, M.; Xu, J.-H.; Pan, Y.; Zhang, Z. *J. Org. Chem.* **2004**, *69*, 5428.
(29) Ruiz, J.; Cutillas, N.; López, F.; López, G.; Bautista, D. *Organometallics* **2006**, *25*, 5768.
(30) Komáromi, A.; Novák, Z. *Chem. Commun.* **2008**, 4968.
(31) John, A.; Shaikh, M. M.; Gosh, P. *Dalton Trans.* **2009**, 10581.
(32) Torborg, C.; Huang, J.; Schulz, T.; Schäffner, B.; Zapf, A.; Spannenberg, A.; Börner, A.; Beller, M. *Chem.—Eur. J.* **2009**, *15*, 1329.
(33) For selected papers on Sonogashira reactions under both Cu-free and ligand-free conditions, see: Liang, B.; Dai, M.; Chen, J.; Yang, Z. *J. Org. Chem.* **2005**, *70*, 391 , and reference 34.
(34) Li, J.-H.; Liang, Y.; Xie, Y.-X. *J. Org. Chem.* **2005**, *70*, 4393.
(35) For a paper on a Sonogashira reaction under both Cu-free and solvent-free conditions, see: Carpita, A.; Ribecai, A. *Tetrahedron Lett.* **2009**, *50*, 204.
(36) For a paper on a Sonogashira reaction under Cu-free, amine-free and ligand-free conditions, see: Urgaonkar, S.; Verkade, J. G. *J. Org. Chem.* **2004**, *69*, 5752.
(37) For a paper on a Sonogashira reaction under Cu-free, amine-free and solvent-free conditions, see: Liang, Y.; Xie, Y.-X.; Li, J.-H. *J. Org. Chem.* **2006**, *71*, 379.
(38) Heck, F.; Dieck, H. A. *J. Organomet. Chem.* **1975**, *93*, 259.
(39) Amatore, C.; Bensalem, S.; Ghalem, S.; Jutand, A.; Medjour, Y. *Eur. J. Org. Chem.* **2004**, 366.
(40) Tougerti, A.; Negri, S.; Jutand, A. *Chem.—Eur. J.* **2007**, *13*, 666.
(41) Ljungdahl, T.; Bennur, T.; Dallas, A.; Emtenäs, H.; Mårtensson, J. *Organometallics* **2008**, *27*, 2490.
(42) Chen, L.-P.; Hong, S.-G.; Huo, H.-Q. *Chin. J. Struct. Chem.* **2008**, *27*, 1404.
(43) Sikk, L.; Tammiku-Taul, J.; Burk, P. *Organometallics* **2011**, *30*, 5656.
(44) Besora, M.; Braga, A. A. C.; Ujaque, G.; Maseras, F.; Lledós, A. *Theor. Chem. Acc.* **2011**, *128*, 639.
(45) Braga, A. A. C.; Ujaque, G.; Maseras, F. *Organometallics* **2006**, *25*, 3647.
(46) Casado, A. L.; Espinet, P. *Organometallics* **1998**, *17*, 954.
(47) García-Melchor, M.; Fuentes, B.; Lledós, A.; Casares, J. A.; Ujaque, G.; Espinet, P. *J. Am. Chem. Soc.* **2011**, *133*, 13519.
(48) Beaupérin, M.; Fayad, E.; Amardeil, R.; Cattey, H.; Richard, P.; Brandès, S.; Meunier, P.; Hierso., J.-C. *Organometallics* **2008**, *27*, 1506.
(49) Beaupérin, M.; Job, A.; Cattey, H.; Royer, S.; Meunier, P.; Hierso., J.-C. *Organometallics* **2010**, *29*, 2815.
(50) This was also confirmed by optimizing the full system in dichloromethane starting with the phenylacetylide at 4 Å far from the cationic complex **I-1**.
(51) Theoretical calculation of the TOF using the scheme developed by Kozuch et al. by means of the AUTOF program shows that the ratio between the anionic and the ionic mechanisms is 2:1 for R = H. This result indicates that both mechanisms are competitive. See refs 52−54.
(52) Kozuch, S.; Shaik, S. *J. Am. Chem. Soc.* **2006**, *128*, 3355.
(53) Kozuch, S.; Shaik, S. *J. Phys. Chem. A* **2008**, *112*, 6032.
(54) Uhe, A.; Kozuch, S.; Shaik, S. *J. Comput. Chem.* **2011**, *32*, 978.
(55) The 2:1 ratio between the base and the alkyne in this ionic mechanism is compatible with the reaction conditions used in experimental kinetic studies, where 6 equiv of base are employed (see Experimental Details section).
(56) For the conversion/time data of the reactions with the different 4-substituted phenylacetylenes, see Supporting Information.
(57) Becke, A. D. *J. Chem. Phys.* **1993**, *98*, 5648.
(58) Lee, C.; Yang, W.; Parr, R. G. *Phys. Rev.* **1988**, *B37*, 785.
(59) Frisch, M. J.; Trucks, G. W.; Schlegel, H. B.; Scuseria, G. E.; Robb, M. A.; Cheese-man, J. R.; Montgomery, J. A., Jr.; Vreven, T.; Kudin, K. N.; Burant, J. C.; Millam, J. M.; Iyengar, S. S.; Tomasi, J.; Barone, V.; Mennucci, B.; Cossi, M.; Scalmani, G.; Rega, N.; Petersson, G. A.; Nakatsuji, H.; Hada, M.; Ehara, M.; Toyota, K.; Fukuda, R.; Hasegawa, J.; Ishida, M.; Nakajima, T.; Honda, Y.; Kitao, O.; Nakai, H.; Klene, M.; Li, X.; Knox, J. E.; Hratchian, H. P.; Cross, J. B.; Bakken, V.; Adamo, C.; Jaramillo, J.; Gomperts, R.; Stratmann, R. E.; Yazyev, O.; Austin, A. J.; Cammi, R.; Pomelli, C.; Ochterski, J. W.; Ayala, P. Y.; Morokuma, K.; Voth, G. A.; Salvador, P.; Dannenberg, J. J.; Zakrzewski, V. G.; Dapprich, S.; Daniels, A. D.; Strain, M. C.; Farkas, O.; Malick, D. K.; Rabuck, A. D.; Raghavachari, K.; Foresman, J. B.; Ortiz, J. V.; Cui, Q.; Baboul, A. G.; Clifford, S.; Cioslowski, J.; Stefanov, B. B.; Liu, G.; Liashenko, A.; Piskorz, P.; Komaromi, I.; Martin, R. L.; Fox, D. J.; Keith, T.; Al-Laham, M. A.; Peng, C. Y.; Nanayakkara, A.; Challacombe, M.; Gill, P. M. W.; Johnson, B.; Chen, W.; Wong, M. W.; Gonzalez, C.; Pople, J. A. *Gaussian 03*, Revision E.01; Gaussian, Inc.: Wallingford, CT, 2004.
(60) Andrae, D.; Häussermann, U.; Dolg, M.; Stoll, H.; Preuss, H. *Theor. Chim. Acta.* **1990**, *77*, 123.
(61) Ehlers, A. W.; Böhme, M.; Dapprich, S.; Gobbi, A.; Höllwarth, A.; Jonas, V.; Köhler, K. F.; Stegmann, R.; Veldkamp, A.; Frenking, G. *Chem. Phys. Lett.* **1993**, *208*, 111.
(62) Höllwarth, A.; Böhme, M.; Dapprich, S.; Ehlers, A. W.; Gobbi, A.; Jonas, V.; Köhler, K. F.; Stegmann, R.; Veldkamp, A.; Frenking, G. *Chem. Phys. Lett.* **1993**, *208*, 237.
(63) Check, C. E.; Faust, T. O.; Bailey, J. M.; Wright, B. J.; Gilbert, T. M.; Sunderlin, L. S. *J. Phys. Chem. A* **2001**, *105*, 8111.
(64) Nova, A.; Ujaque, G.; Maseras, F.; Lledós, A.; Espinet, P. *J. Am. Chem. Soc.* **2006**, *128*, 14571.
(65) Álvarez, R.; Pérez, M.; Faza, O. N.; de Lera, A. R. *Organometallics* **2008**, *27*, 3378.
(66) Ariafard, A.; Yates, B. F. *J. Am. Chem. Soc.* **2009**, *131*, 13981.
(67) Pérez-Rodríguez, M.; Braga, A. A. C.; García-Melchor, M.; Pérez-Temprano, M. H.; Casares, J. A.; Ujaque, G.; de Lera, A. R.; Álvarez, R.; Maseras, F.; Espinet, P. *J. Am. Chem. Soc.* **2009**, *131*, 3650.
(68) Pérez-Rodríguez, M.; Braga, A. A. C.; de Lera, A. R.; Maseras, F.; Álvarez, R.; Espinet, P. *Organometallics* **2010**, *29*, 4983.
(69) Thaler, T.; Haag, B.; Gavryushin, A.; Schober, K.; Hartmann, E.; Gschwind, R. M.; Zipse, H.; Mayer, P.; Knochel, P. *Nat. Chem.* **2010**, *2*, 125.

(70) Following the argument in: Martin, R. L.; Hay, P. J.; Pratt, L. R. *J. Phys. Chem. A* **1998**, *102*, 3565 , and its application in reference 71.
(71) Sieffert, N.; Bühl, M. *J. Am. Chem. Soc.* **2010**, *132*, 8056.
(72) Miertus, S.; Scrocco, E.; Tomasi, J. *J. Chem. Phys.* **1981**, *55*, 117.
(73) Mao, J.; Xie, G.; Wu, M.; Guo, J.; Ji, S. *Adv. Synth. Catal.* **2008**, *350*, 2477.
(74) Wan, Z.; Jones, C. D.; Mitchell, D.; Pu, J. Y.; Zang, T. Y. *J. Org. Chem.* **2006**, *71*, 826.
(75) Polshettiwar, V.; Nadagouda, M. N.; Varma, R. S. *Chem. Commun.* **2008**, 6318.